NANO LETTERS

Letter

pubs.acs.org/NanoLett

Nanoscale Limitations in Metal Oxide Electrocatalysts for Oxygen Evolution

Venkatasubramanian Viswanathan,[†,‡,§,∥] Katie L. Pickrahn,[†,∥] Alan C. Luntz,[‡] Stacey F. Bent,[†] and Jens K. Nørskov*[,†,‡]

[†]Department of Chemical Engineering, Stanford University, Stanford, California 94305-5025, United States

[‡]SUNCAT, SLAC National Accelerator Laboratory, Menlo Park, California 94025-7015, United States

[§]Department of Mechanical Engineering, Carnegie Mellon University, Pittsburgh, Pennsylvania 15213, United States

Supporting Information

ABSTRACT: Metal oxides are attractive candidates for low cost, earth-abundant electrocatalysts. However, owing to their insulating nature, their widespread application has been limited. Nanostructuring allows the use of insulating materials by enabling tunneling as a possible charge transport mechanism. We demonstrate this using TiO_2 as a model system identifying a critical thickness, based on theoretical analysis, of about ∼4 nm for tunneling at a current density of ∼1 mA/cm^2. This is corroborated by electrochemical measurements on conformal thin films synthesized using atomic layer deposition (ALD) identifying a similar critical thickness. We generalize the theoretical analysis deriving a relation between the critical thickness and the location of valence band maximum relative to the limiting potential of the electrochemical surface process. The critical thickness sets the optimum size of the nanoparticle oxide electrocatalyst and this provides an important nanostructuring requirement for metal oxide electrocatalyst design.

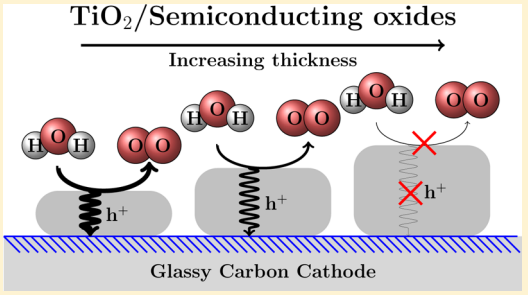

KEYWORDS: *Charge transport, nanostructuring, atomic layer deposition, water splitting*

Electrochemical and photoelectrochemical processes such as the splitting of water to hydrogen and oxygen form key routes toward the storage of renewable electricity in the form of chemical bonds.[1,2] Metal oxides, owing to their high stability under oxygen-evolving conditions and low cost are the material of choice for catalyzing the oxygen evolution reaction (OER), an important half reaction in many of these electrochemical and photoelectrochemical processes.[3] However, electrocatalysts must also allow charge transport to the active site. This can be a major limitation for many metal oxides such as some NiO_x, MnO_x, and transition metal-doped TiO_2, that possess limited electronic conductivity but may have good electrocatalytic activity.[4−7] Nanostructuring offers a potential solution by lowering the distance required for the charge to travel and allowing for additional charge transport mechanisms such as tunneling to become active. Here, we present an analysis allowing an estimate of the material-dependent critical thickness beyond which charge transport significantly affects the electrochemistry.

In semiconducting materials, there are many possible mechanisms of charge transport, including hopping of polarons, transport at defects, and transport via grain boundaries. However, all are limited in the current they can support. We use TiO_2 as a model system to illustrate the role of charge transport in oxide materials. Bulk TiO_2 is a semiconductor with a band gap of about 3.2 eV.[8] While expected to be a poor catalyst for OER, TiO_2 was utilized because its electronic properties (band positions, low conductivity) may be used to model more active semiconducting catalysts. It has low ionic conductivity,[9] allowing us to more directly probe electron transport.[10] In addition, understanding the charge transport of TiO_2 itself is of significance because it is an important material in dimensionally stable anodes (DSAs) type electrodes that are often used in industry to catalyze OER[11] and it has recently been used in groundbreaking photoelectrochemical devices as a passivation layer.[12] Despite its importance, charge transport within TiO_2 under OER conditions is still ill defined. While many modes of transport may be active, for sufficiently thin TiO_2, tunneling is operative and can contribute in a dominant way to the charge transport, characteristic of many metal oxide systems. The question is how thin is sufficient? An important factor determining the coherent tunneling rate is the position of the valence and conduction bands relative to the relevant redox potential for the reaction of interest. A schematic of the bulk band levels of TiO_2 along with important redox potentials are marked in Figure 1a relative to the vacuum reference. It can be immediately seen that the equilibrium potential for oxygen evolution is in the band gap of TiO_2. The thermodynamic limiting potential, U^{OER}, defined as the potential at which the reaction scheme for oxygen evolution is downhill in free energy,

Received: July 21, 2014
Revised: September 5, 2014
Published: September 12, 2014

   dx.doi.org/10.1021/nl502775u | *Nano Lett.* 2014, 14, 5853−5857

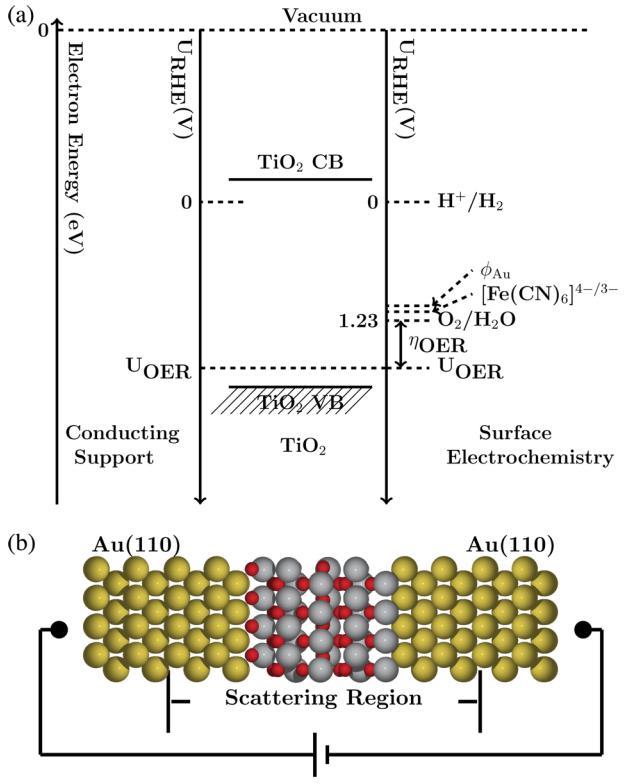

Figure 1. (a) Sketch of the electronic structure for the TiO_2 catalysts and electrolyte. Plotted are the redox positions of the band positions for O_2/H_2O and $[Fe(CN)_6]^{3-/4-}$ as calculated for the experimental conditions in this report (pH 7 for $[Fe(CN)_6]^{3-/4-}$ and pH 13 for H_2O/O_2) and the work function of Au. The close proximity of the redox potential of $[Fe(CN)_6]^{3-/4-}$ and the work function of Au to the redox potential of O_2/H_2O work function indicate that they are good estimates for probing the electronic conductivity of TiO_2 under OER conditions. (b) Structure of the MIM configuration used to probe the electronic conductivity of TiO_2. The MIM configuration consists of Au leads on either side with the scattering region consisting of Au|TiO_2|Au.

is the potential at which we would expect a large reaction rate for oxygen evolution on TiO_2.[7] On the basis of the locations of the band levels of TiO_2,[13] we expect the thermodynamic limiting potential for oxygen evolution reaction, U^{OER}, is also in the band gap of TiO_2, located close to the valence band.

To probe the coherent charge transport of TiO_2 under the operating electrochemical conditions, we need to mimic the conducting support/TiO_2/electrolyte interface. On the basis of the energy diagram shown in Figure 1a, it can be seen that there is a well-defined chemical potential at the semiconductor-electrolyte interface set by the limiting potential for onset of oxygen evolution, U^{OER}. The conducting support, glassy carbon, is modeled using a gold electrode as they possess similar work functions. We have chosen gold to model the semiconductor–electrolyte interface as the work function is in the range of the potential for oxygen evolution (Figure 1b). The electrochemical system is modeled using a metal–insulator–metal (MIM) configuration in a similar manner as used to study Li_2O_2 charge transport.[14] All charge transport calculations are performed using density functional theory along with a Hubbard-U correction as implemented in the GPAW package. Full details can be found in the Supporting Information.

Transport calculations are carried out at different thicknesses of the TiO_2 film. At a fixed constant bias, U_{bias}, applied across the TiO_2 film, we observe an exponential drop in the maximum tunneling current density, j_t, with increasing thickness, d, as shown in Supporting Information Figure S6b. A necessary requirement for the electrochemistry at the solid–liquid interface is that j_t is sufficient to sustain the electrochemical current. A current density at a given potential can be determined using the Tafel expression. Thus, the overall current invoking the charge transport requirement can be calculated as

$$j = j_0 \min\left(\exp\left\{-\frac{(U - U_{bias} - U^{rxn})}{kT}\right\}, 1\right) \Big| [j_t(U_{bias}) = j] \quad (1)$$

where j_0 represents the exchange current density, U^{rxn} represents the redox potential, U_{bias} represents the minimum bias required across the film to sustain the electrochemical current, j, and U is the applied potential. Here, we have assumed a transfer coefficient of 1 for the Tafel kinetics. When the potential has been increased past the redox potential, U^{rxn}, the proton transfer becomes exergonic and it has been shown that this correlates well with the potential where the current density loses its potential dependence and is given by its prefactor, j_0.[15,16] This is expressed by the minimum condition that enforces that when $U > (U^{rxn} + U_{bias})$ the electrochemical current density, j, is equal to the exchange current density, j_0. From eq 1 and Supporting Information Figure S6b, it is clear that below a limiting thickness, the electrocatalytic activity should remain unchanged as only a very small bias is sufficient to drive the required electrochemical current. However, beyond the limiting thickness, there is an increase in bias, U_{bias}, required to sustain the electrochemical current. The bias potential, U_{bias}, is in series with the overpotential driving the electrochemical reaction as given by eq 1. In a potentiostatic experiment, this additional bias required would appear as an apparent decrease in current. The results of j as a function of thickness, d, for a redox couple is shown in Figure 2. The electrochemical current

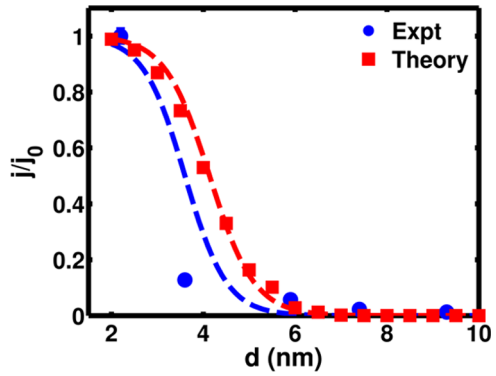

Figure 2. Theoretical and experimental plot of the extracted kinetic current density of the $[Fe(CN)_6]^{3-/4-}$ redox couple as a function of thickness at a fixed potential U_{RHE} = 1.2 V (U^o $(Fe(CN)_6]^{3-/4-}$ = 0.87 V_{RHE}, η = 0.33 V). The theoretical analysis is based on including the charge transport limitations as a function of thickness using MIM calculations shown in the Supporting Information. The experimental data points are from rotating disk electrode experiments carried out at 1600 rpm. The error bars of the extracted experimental kinetic current density are associated with the uncertainties in estimating the diffusion-limited current density. The calculated theoretical curve includes a roughness of about 0.5 nm, typical of ALD growth for TiO_2. The dashed lines are best-fit lines for the data points.

dx.doi.org/10.1021/nl502775u | Nano Lett. 2014, 14, 5853–5857

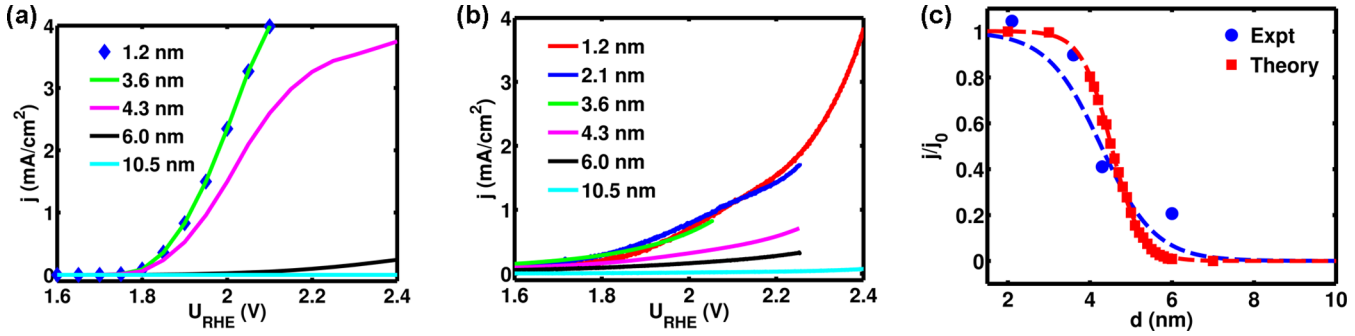

Figure 3. Comparison of theoretical (a) and experimental (b) linear sweep voltammogramms for OER on different thicknesses of TiO_2 thin films. The theoretical and experimental data follow similar trends. The activity of films thicker than ~4 nm decreases with increasing thickness due to an increase in the bias potential required to sustain the electrochemical current. This trend can be more clearly seen in (c), comparing the theory and experimental data for the current density at 2.0 V, during which OER occurs. The current density is normalized by the current obtained at 2.0 V for the 1.2 nm TiO_2 sample and the calculated polarization curve includes a roughness of about 0.5 nm, typical of ALD growth for TiO_2.

is normalized by the current at a thickness 2.1 nm to enable quantitative comparisons with an experimental probe discussed below. On the basis of the analysis, we identify a critical thickness of about 4 nm, beyond which charge transport becomes limiting for TiO_2.

To validate this picture, we need an in situ experimental probe of the electronic conductivity of TiO_2 under the operating electrochemical conditions. Here, we employ the technique of using a reversible "outer-sphere" redox couple to measure the operando electronic conductivity. As discussed above, the probe redox couple chosen must have a redox potential in the range of oxygen evolution.[17−20] $[Fe(CN)_6]^{3-/4-}$ was chosen as the probe redox couple satisfying this criteria as illustrated in Figure 1a. To examine the thickness dependence, TiO_2 films are deposited on polished glassy carbon electrodes using ALD. ALD allows for the deposition of conformal thin films with high control of thickness and uniformity and is increasingly utilized in the field of catalysis.[21−23] The thickness is controlled by the number of ALD cycles (see Supporting Information). While the exact mechanism of growth on the glassy carbon is not known, even for the thinnest samples tested (~1 nm) consisted of more than 40 ALD cycles and showed significant amount of TiO_2 by XPS. The kinetic current density from the oxidation of $[Fe(CN)_6]^{4-}$ at 1.2 V_{RHE} while spinning at 1600 rpm is extracted using the Koutecky−Levich equation and plotted for different thicknesses in Figure 2 (see Supporting Information). The current due to the redox reaction of $[Fe(CN)_6]^{3-/4-}$ at a fixed potential shows a strong dependence on the thickness of TiO_2 with a rapid decay observed with increasing film thickness around 4 nm. To enable a quantitative comparison of the experimental and theoretical analysis, we must include the effects of roughness. We expect the films deposited by ALD to have a RMS roughness between 0.5 to 1 nm.[24] This is included in the theoretical analysis by using a normal distribution with the width of the distribution given by the RMS roughness.

The results obtained from the theoretical and experimental analysis of charge transport for TiO_2 have important implications on the electrocatalytic activity for OER. Similar to the redox couple analysis discussed above, OER occurring at the semiconductor−electrolyte interface requires that the rate associated with the charge transport, j_t, is sufficient to support the electrochemical current, j. In this case, $U^{rxn} = U^{OER}$, which is the calculated limiting potential based on density functional theory calculations. When the potential is increased beyond U^{OER}, the proton transfer becomes exergonic, and is given by its prefactor, j_0.[15] The theoretical cyclic voltammograms for TiO_2 derived from this analysis are shown in Figure 3a and display this trend, with a limiting thickness ~4 nm.

To validate these predictions, TiO_2 films with thicknesses between 1.2 and 10.5 nm are tested as catalysts for OER using cyclic voltammetry (CV). Electrochemical testing is carried out in a rotating disk electrode (RDE) configuration and the anodic-going direction of the first CV sweep for different thicknesses is plotted in Figure 3b. The samples indeed display the two unique behaviors described above. Thin samples (<4 nm thick) all show similar activity, although as expected the results show that TiO_2 is poor at catalyzing oxygen evolution. The OER activity of samples thicker than 4 nm decreases with increasing thickness due to the charge transport limitations. High-resolution XPS did not show any significant difference in the Ti-2p peak positions between a 1.1 and 10.5 nm TiO_2 film deposited on glassy carbon (see Supporting Information). This suggests that there are not significant differences in the electronic state of the TiO_2 with film thickness.

For a more quantitative comparison, the current density obtained at 2.0 V versus the thickness of TiO_2 for both the experimental and theoretical OER CVs is plotted in Figure 3c. In order to compare the distance dependence, we normalize both the experimental and theoretical data to the current density obtained at 2.0 V for the 1.2 nm TiO_2 electrode. We see a drop off in current density on similar length scales between the theoretical and experimental data. A roughness of about 1 nm is included in the theoretical simulations as described above, and the rate of decay predicted by theory is in close agreement with that observed experimentally. Further, both theory and experiment identify a limiting thickness of ~4 nm.

Having established an understanding of the role of electron transport and the associated limiting thickness of TiO_2 nanostructures for OER, we now generalize this analysis to describe the limiting thickness supported by tunneling for other insulating oxide materials. As illustrated in Figure 1a, the barrier height for tunneling is determined by the location of the valence band level relative to the theoretical limiting potential for oxygen evolution, U_{OER}, on that material. The detailed MIM calculations described here for TiO_2 can be approximated using the well-known Simmons formula for charge transport.[25] The Simmons formula assumes a trapezoidal tunneling barrier and applies a simple WKB approximation for tunneling. The tunneling current is given by

dx.doi.org/10.1021/nl502775u | Nano Lett. 2014, 14, 5853−5857

$$j_t = j_0(\phi e^{-A\sqrt{\phi}\,d} - (\phi + eU_{bias})e^{-A\sqrt{(\phi+eU_{bias})}\,d}) \quad (2)$$

where j_0 is the prefactor, $\phi = U_{VBM} - U_{OER}$ is the barrier height, and $A = 4\pi\beta/h(2m)^{1/2}$. β is a correction factor typically ~1 and m is the tunneling mass (assumed here to be the mass of the electron). Using this relation, we can calculate the limiting thickness, d, as a function of the barrier height for a fixed current density and this is shown in Figure 4 for j = 10, 1, 0.01 mA/cm^2. The prefactor, j_0, to be used in the Simmons formula in eq 2, is chosen based on the detailed nonequilibrium Green's function (NEGF) MIM calculations carried out for TiO_2. The obtained prefactor is close to the simple Simmons estimate, $j_0 = e/(2\pi h(\beta d)^2)$. We find that changes in current density have a minimal effect on the limiting thickness. We also include the experimental thickness dependent data for TiO_2 from this work and CoO_x from the work of Yeo et al.[26] In our calculations, the location of the valence band relative to the redox potential for oxygen evolution is estimated based on our theoretical MIM calculations for TiO_2 and Co_3O_4 (see Supporting Information). While Yeo et al. suggest that the differences in catalytic activity are attributable to changes in the oxidation state of the CoO_x, here, we look at the effects if the electronic conductivity also plays a role. We note though, that in the Yeo et al. work, the CoO_x was electrodeposited, which may introduce some porosity that increases the observed value of the critical thickness (we observed a similar increase in the critical thickness of ALD TiO_2 that contained a CVD component which also likely had enhanced porosity). This is consistent with the slight underestimate in our calculations for the CoO_x. On the basis of the assumption that electronic conductivity could be limiting, the theoretical prediction for CoO_x agrees reasonably with the experimental data. However, the actual observed particle size effect for CoO_x could be due to a combination of these factors and this requires further investigations.

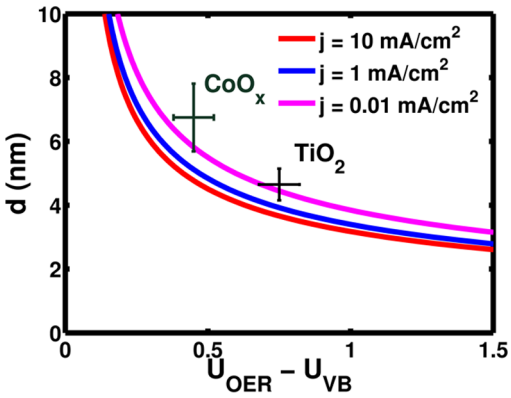

Figure 4. A plot of d as a function of the barrier height given by ($U_{OER} - U_{VB}$). The theoretical lines for current density j = 10, 1, 0.01 mA/cm^2 are calculated based on the Simmons formula for charge transport. The location of the valence band maximum relative to U_{OER} for TiO_2 and Co_3O_4 are estimated based on the density of states plot shown in Supporting Information. The experimental limiting thickness for TiO_2 is based on this work and that for CoO_x is based on the work of Yeo et al.[26]

The critical thickness calculated for tunneling current from our analysis should serve as a condition beyond which charge transport must be considered. Theoretical calculations have predicted multiple active OER catalysts that have yet to be fully realized possibly due to the masking effects of charge transport limitations.[6] In addition, the charge transport effects may be present in layered systems where the active surface is on a wide-band gap material (e.g., MnO_x on MnO or RuO_x on TiO_2[27]). Thin films are drawing increasing attention as a method to evaluate catalysts' intrinsic activity,[28] and this work can be used to provide guidance to the minimum thickness needed for these films. Proper consideration of charge transport may also help correctly identify factors that enhance activity. For example, the role of Fe in Ni–Fe oxide OER catalysts had long been identified as a method to enhance the conductivity of NiO_x films but has recently been identified as a major contributor to the intrinsic activity.[29] The study carried out by Trotochaud et al. reiterates the importance of decoupling the in situ electronic conductivity and the intrinsic catalytic activity.[29] Alternative charge transport mechanisms such as ion-transport through a porous thin film may allow for larger critical thicknesses and likely depends on the deposition method; however, the effect of film thickness will become increasingly important to consider when dense thin films are used, such as those deposited by ALD.

In this work, we have studied the role of nanostructuring in electrocatalysis as a way to overcome the charge transport limitations faced by materials with low electronic conductivity. We have utilized TiO_2 as a model system to explore the role of coherent tunneling as the mode of charge transport. On the basis of theory calculations in a MIM structure, we show that there is a rapid decay in operando electronic conductivity with thickness of TiO_2. These calculations are in good agreement with electronic conductivity measured using a redox couple on well-defined TiO_2 films prepared by ALD. These charge transport limitations have important implications for electrocatalysis and beyond a certain limiting thickness, a bias potential is required to sustain the electrochemical current. This bias potential appears as an apparent increase in the overpotential for oxygen evolution. We observed the masking effect charge transport limitations using both theoretical simulations and experimental RDE measurements on well-defined TiO_2 films. Finally, we generalize the analysis to provide a relation between this limiting thickness for charge transport to the location of the valence band relative to the limiting potential for OER. This relation offers a guideline for nanostructuring requirements to enable traditionally insulating materials as thin film electrocatalysts.

■ ASSOCIATED CONTENT

Supporting Information

Methods, ALD TiO_2 characterization, calculation of mass transport limited current, impact of charge transport limitations on other catalysts, computational method details, and projected density of states of TiO_2 and that of Co_3O_4. This material is available free of charge via the Internet at http://pubs.acs.org.

■ AUTHOR INFORMATION

Corresponding Author

*E-mail: norskov@stanford.edu.

Author Contributions

[||]V.V and K.L.P contributed equally to this work.

V.V, K.L.P., S.F.B, and J.K.N designed the research. V.V. performed the theoretical calculations. K.L.P. performed the experiments. V.V., K.L.P., A.C.L., S.F.B, and J.K.N. cowrote the manuscript.

Notes

The authors declare no competing financial interest.

■ ACKNOWLEDGMENTS

This work was supported as part of the Center on Nanostructuring for Efficient Energy Conversion (CNEEC), an Energy Frontier Research Center funded by the U.S. Department of Energy, Office of Science, Basic Energy Sciences under Award # DE-SC0001060. K.L.P. acknowledges a graduate fellowship through the NSF. The authors would like to acknowledge helpful discussions with Aleksandra Vojvodic, Blaise Pinaud, and Mónica García-Mota.

■ REFERENCES

(1) Lewis, N. S.; Nocera, D. G. *Proc. Natl. Acad. Sci. U.S.A.* **2006**, *103* (43), 15729−15735.
(2) Walter, M. G.; Warren, E. L.; McKone, J. R.; Boettcher, S. W.; Mi, Q. X.; Santori, E. A.; Lewis, N. S. *Chem. Rev.* **2010**, *110* (11), 6446−6473.
(3) Katsounaros, I.; Cherevko, S.; Zeradjanin, A. R.; Mayrhofer, K. J. J. *Angew. Chem., Int. Ed.* **2014**, *53* (1), 102−121.
(4) Trasatti, S. *Electrochim. Acta* **1991**, *36* (2), 225−241.
(5) Trotochaud, L.; Ranney, J. K.; Williams, K. N.; Boettcher, S. W. *J. Am. Chem. Soc.* **2012**, *134* (41), 17253−17261.
(6) Garcia-Mota, M.; Vojvodic, A.; Metiu, H.; Man, I. C.; Su, H. Y.; Rossmeisl, J.; Norskov, J. K. *ChemCatChem* **2011**, *3* (10), 1607−1611.
(7) Man, I. C.; Su, H. Y.; Calle-Vallejo, F.; Hansen, H. A.; Martinez, J. I.; Inoglu, N. G.; Kitchin, J.; Jaramillo, T. F.; Norskov, J. K.; Rossmeisl, J. *ChemCatChem* **2011**, *3* (7), 1159−1165.
(8) Ni, M.; Leung, M. K. H.; Leung, D. Y. C.; Sumathy, K. *Renewable Sustainable Energ Rev.* **2007**, *11* (3), 401−425.
(9) Chen, Y. W.; Prange, J. D.; Duhnen, S.; Park, Y.; Gunji, M.; Chidsey, C. E. D.; McIntyre, P. C. *Nat. Mater.* **2011**, *10* (7), 539−544.
(10) Doyle, R. L.; Godwin, I. J.; Brandon, M. P.; Lyons, M. E. G. *Phys. Chem. Chem. Phys.* **2013**, *15* (33), 13737−13783.
(11) Trasatti, S. *Electrochim. Acta* **2000**, *45* (15−16), 2377−2385.
(12) Hu, S.; Shaner, M. R.; Beardslee, J. A.; Lichterman, M.; Brunschwig, B. S.; Lewis, N. S. *Science* **2014**, *344* (6187), 1005−1009.
(13) Xu, Y.; Schoonen, M. A. A. *Am. Mineral.* **2000**, *85* (3−4), 543−556.
(14) Viswanathan, V.; Thygesen, K. S.; Hummelshoj, J. S.; Norskov, J. K.; Girishkumar, G.; McCloskey, B. D.; Luntz, A. C. *J. Chem. Phys.* **2011**, *135* (21), 214704.
(15) Norskov, J. K.; Rossmeisl, J.; Logadottir, A.; Lindqvist, L.; Kitchin, J. R.; Bligaard, T.; Jonsson, H. *J. Phys. Chem. B* **2004**, *108* (46), 17886−17892.
(16) Viswanathan, V.; Nørskov, J. K.; Speidel, A.; Scheffler, R.; Gowda, S.; Luntz, A. C. *J. Phys. Chem. Lett.* **2013**, *4* (4), 556−560.
(17) Heusler, K. E.; Yun, K. S. *Electrochim. Acta* **1977**, *22* (9), 977−986.
(18) Klahr, B. M.; Hamann, T. W. *J. Phys. Chem. C* **2011**, *115* (16), 8393−8399.
(19) Stoerzinger, K. A.; Risch, M.; Suntivich, J.; Lu, W. M.; Zhou, J.; Biegalski, M. D.; Christen, H. M.; Ariando; Venkatesan, T.; Shao-Horn, Y. *Energ Environ. Sci.* **2013**, *6* (5), 1582−1588.
(20) Macpherson, J. V.; de Mussy, J. P. G.; Delplancke, J. L. *J. Electrochem. Soc.* **2002**, *149* (7), B306−B313.
(21) George, S. M. *Chem. Rev.* **2010**, *110* (1), 111−131.
(22) Stair, P. C. *Top Catal.* **2012**, *55* (1−2), 93−98.
(23) Peng, Q.; Lewis, J. S.; Hoertz, P. G.; Glass, J. T.; Parsons, G. N. *J. Vac Sci. Technol., A* **2012**, *30* (1), 010803.
(24) McDaniel, M. D.; Posadas, A.; Wang, T.; Demkov, A. A.; Ekerdt, J. G. *Thin Solid Films* **2012**, *520* (21), 6525−6530.
(25) Luntz, A. C.; Viswanathan, V.; Voss, J.; Varley, J. B.; Norskov, J. K.; Scheffler, R.; Speidel, A. *J. Phys. Chem. Lett.* **2013**, *4* (20), 3494−3499.
(26) Yeo, B. S.; Bell, A. T. *J. Am. Chem. Soc.* **2011**, *133* (14), 5587−5593.
(27) Morita, M.; Iwakura, C.; Tamura, H. *Electrochim. Acta* **1978**, *23* (4), 331−335.
(28) Trotochaud, L.; Boettcher, S. W. *Scr. Mater.* **2014**, *74*, 25−32.
(29) Trotochaud, L.; Young, S. L.; Ranney, J. K.; Boettcher, S. W. *J. Am. Chem. Soc.* **2014**, *136* (18), 6744−6753.